Three-dimensional particle-in-cell simulation of discharge characteristics in cylindrical anode layer hall plasma accelerator

S. F. Geng,[1] X. M. Qiu,[1] C. M. Cheng,[1] Paul. K. Chu,[2] and D. L. Tang[1,a)]
[1]*Southwestern Institute of Physics, Chengdu 610041, China*
[2]*Department of Physics and Materials Science, City University of Hong Kong, Tat Chee Avenue, Kowloon, Hong Kong, China*

(Received 23 December 2011; accepted 27 March 2012; published online 25 April 2012)

A current drop is found when the discharge voltage is increased in the cylindrical anode layer hall plasma accelerator and three-dimensional particle-in-cell simulation is performed to investigate the phenomenon. The simulation results which agree with experiments show that the ion density in the discharge region does not always rise when the discharge voltage is increased and the ion density reaches a maximum value at the appropriate voltage. This phenomenon is considered to be the macroscopic ramification of the change in the ionization cross section as the electron energy varies. With regard to Ar^+, the largest ionization cross section appears when the electron energy is 45–110 eV. In the hall plasma accelerator, the electron drift speed is governed by E/B and controls the electron energy. Finally, the cross section of producing Ar^+ is determined by E/B. Our analysis reveals that the proper E/B value in the ionization region is 2.81×10^6 m/s to 4.40×10^6 m/s for argon. © *2012 American Institute of Physics*. [http://dx.doi.org/10.1063/1.3703321]

I. INTRODUCTION

In a hall plasma accelerator which is a type of gas discharge device originating from research in electric propulsion, electrons experience a closed drift in the $\vec{E} \times \vec{B}$ direction called hall drift and the drift speed is E/B. Since ions are accelerated in the quasi-neutral plasma, they are not subject to the space charge limitation. A hall plasma accelerator is usually of either the magnetic layer type or anode layer type. A magnetic layer hall plasma accelerator consists of a ceramic wall as the discharge channel and the discharge channel is long compared to the channel width. Hence, it is also called a hall plasma accelerator with an extended dielectric channel. On the other hand, an anode layer hall plasma accelerator has a conducting wall as the discharge channel, and the channel is short compared to the channel width. In the anode layer hall plasma accelerator, electrons do not collide with the metal wall and so they have high energy as they get to the zone near the anode. This causes a sharp increase in the plasma potential and many ions are formed and accelerated in this zone, thereby giving the name "anode layer."[1–3] The anode layer hall plasma accelerator has either the circular or linear configuration, both of which are readily scalable, especially the linear one which can be scaled to any designed length.[4] Owing to the simplicity and robustness, the anode layer hall plasma accelerator is suitable for surface modification and thin film fabrication in industrial applications.[5–10] However, there are a few technological aspects that need improvement. For instance, an anode layer hall plasma accelerator with high voltage and high efficiency is welcomed by the industry. In addition, the sputtered cathode materials are unacceptable in many applications and so an anode layer hall plasma accelerator with a small self-etching rate is desirable.

Recently, much effort has been made to model the plasma behavior in hall plasma accelerators by, for example, the fluid model,[11–13] particle-in-cell (PIC) model,[14] and hybrid-PIC model.[15] The near field plume is described by a 2-dimensional (2D) hybrid-PIC model[16] and the interactions between the plasma and wall have been simulated by Sommier *et al.*, also based on a 2D hybrid-PIC model.[17] The sheath formation and expansion have been investigated using a 2D hydrodynamic approach by Keidar *et al.*[18] and the high-frequency electron drift instability by Ducrocq *et al.* using PIC simulation as well.[19] In our investigation of anode layer hall plasma accelerators with both the linear and cylindrical configurations,[20–22] it was found that the discharge current dropped when the discharge voltage exceeded a certain value. This appears to be related to the correlation between the electron energy and ionization cross section. The ionization cross section can affect the plasma accelerator performance significantly. Under the same conditions, different working gases have different cross sections and ionization probability, and so the choice of the working gas has a direct influence on the plasma accelerator efficiency.[23] An anode layer hall plasma accelerator is based on electron ionization (also known as electron impact) and the ionization efficiency depends strongly on the physical properties of the working gas and electron energy. At low energies, the de Broglie wavelength of the electrons is larger than the dimensions of atoms and owing to electron diffraction, the interactions between electrons and gas atoms are insufficient to transfer enough energy for ionization. At the proper energy, the de Broglie wavelength of electrons matches the dimensions of atoms and energy transfer to atoms is maximized, leading to strong ionization. At higher energies, the de Broglie wavelength of the electrons becomes smaller than the

a)Electronic mail: tangdeli@263.net.

 © 2012 American Institute of Physics

atom dimensions. In this case, the atoms become transparent to electrons and the ionization efficiency diminishes. The behavior is exhibited by the correlation between the electron energy and ionization collision cross section. In the anode layer hall plasma accelerator, the electron velocity is governed by E/B and the ionization cross section and ionization probability are determined by E/B.

In the work presented in this paper, we perform three-dimensional (3D) PIC simulation with Monte Carlo collisions (PIC-MCC) to analyze the discharge characteristics of the cylindrical anode layer hall plasma accelerator and provide experimental verification. The paper is organized as follows. In Sec. II, the details of the experiment are presented. Section III describes the numerical simulation and Sec. IV presents the results, analysis, and explanation. The main conclusions are summarized in Sec. V.

II. EXPERIMENTAL DETAILS

The experiments were performed using our ion source test platform. The inside dimension of the vacuum vessel is 625 mm and the length is 2300 mm. The test platform is equipped with two turbomolecular pumps as the main ones. Fig. 1 shows the front view of the cylindrical anode layer hall plasma accelerator. Its outside dimension is 94 mm. Fig. 2 depicts the schematic cross-sectional diagram of the cylindrical anode layer hall plasma accelerator. The outlet dimension of the anode layer hall plasma accelerator is 50 mm and the marked parts will be simulated in Sec. III.

In our experiments, the working gas was argon. As shown in Fig. 3, the discharge current rises as the discharge voltage is increased and then drops when the discharge voltage exceeds 900 V at an argon pressure of 2.0×10^{-2} Pa.

Fig. 3 suggests that there is an optimal voltage for ionization in the plasma accelerator. That is, there is an appropriate discharge voltage to match the magnetic field to obtain the largest discharge current and discharge power.

III. NUMERICAL SIMULATION

The simulation is performed by the 3D particle-in-cell method using the software VORPAL by Tech-X Corporation.

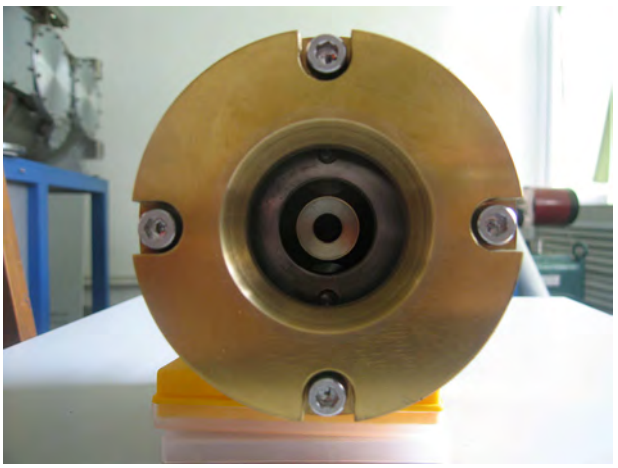

FIG. 1. Front view of the cylindrical anode layer hall plasma accelerator.

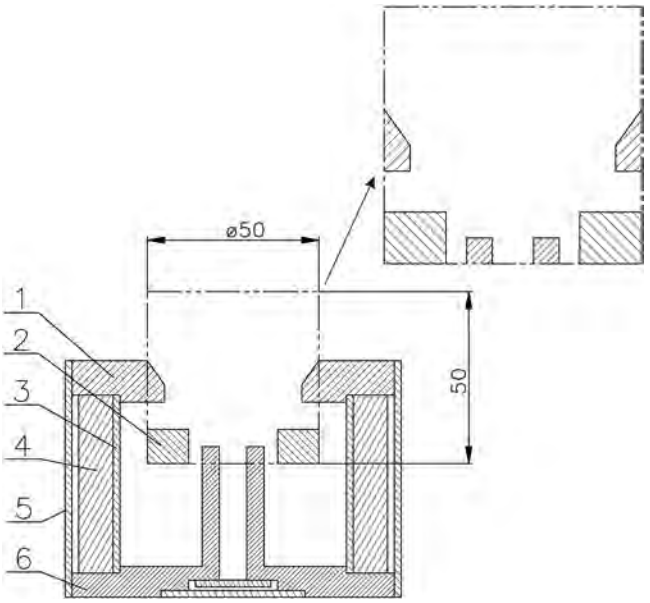

FIG. 2. Schematic cross-sectional diagram of the cylindrical anode layer hall plasma accelerator and simulated parts: (1) cathode/outer magnetic pole, (2) anode, (3) inner shield, (4) permanent magnet, (5) outer shield, and (6) cathode/inner magnetic pole.

The anode layer hall plasma accelerator used in our experiments is schematically illustrated in Fig. 2, and Fig. 4 illustrates the 3D model used in the simulation.

The correlation between the electron energy and ionization cross section for argon described by Wetzel *et al.* and Straub *et al.* is shown in Fig. 5,[24,25] showing that the proper electron energy for argon ionization is about 45–110 eV.

In the simulation, the argon pressure is 2×10^{-2} Pa to be consistent with the experiments. The magnetic field is calculated by the 3D model and particle collision is handled by MCC. The collisions include electron-neutral collisions (ionization, excitation, and elastic scattering) as well as ion-neutral collisions (charge exchange and elastic scattering). We use the ionization cross sections in Refs. 24 and 25 in the simulation, and the other cross section data (excitation collisions, elastic collisions, and ion-neutral collisions) are the VORPAL built-in data. The model is based on the 3D Cartesian coordinates.

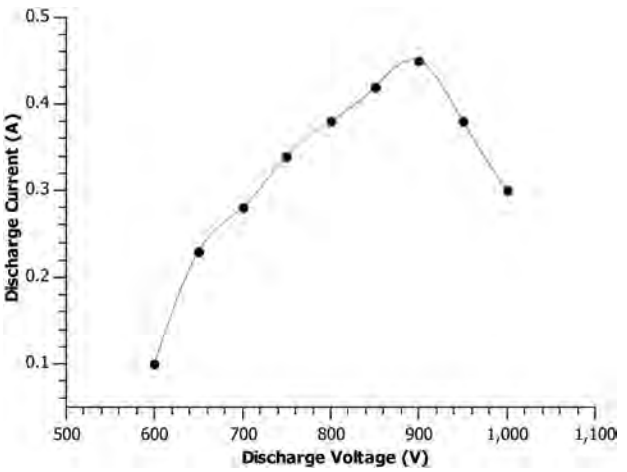

FIG. 3. V-I characteristics of a cylindrical anode layer hall plasma accelerator.

FIG. 4. 3D model used in the simulation.

IV. RESULTS AND DISCUSSION

The general electron and ion distributions in space are shown in Fig. 6. The electrons are confined in the region near the anode (Fig. 6(a)) and meanwhile, ions are formed in this region and accelerated to the exit plane (Fig. 6(b)). The centralized electron distribution indicates the high anode efficiency. Only a very small fraction of ions can reach the cathode surface and so the plasma accelerator exhibits very little self-etching. Furthermore, it indicates that the high $E \times B$ region and ion acceleration region are the regions near the anode surface. Fig. 7 shows the electron drift in this plasma accelerator, confirming that the 3D model is consistent with the physics of a closed-drift plasma accelerator.

In the simulation, the discharge voltage is changed from 400 V to 1200 V and the ion density changes as the discharge voltage is altered. As the discharge voltage is increased, the ion density rises, but when the discharge voltage exceeds 900 V, the ion density diminishes.

Fig. 8 shows that the correlation between the ion density and discharge voltage is the same as the discharge current

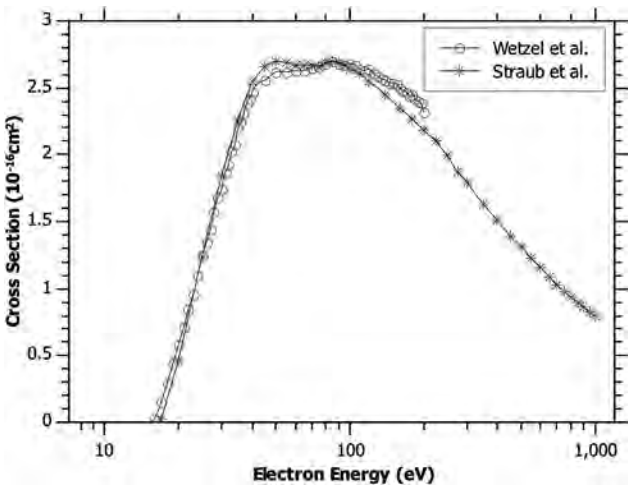

FIG. 5. Cross section of producing Ar^+ versus electron energy (Refs. 24 and 25).

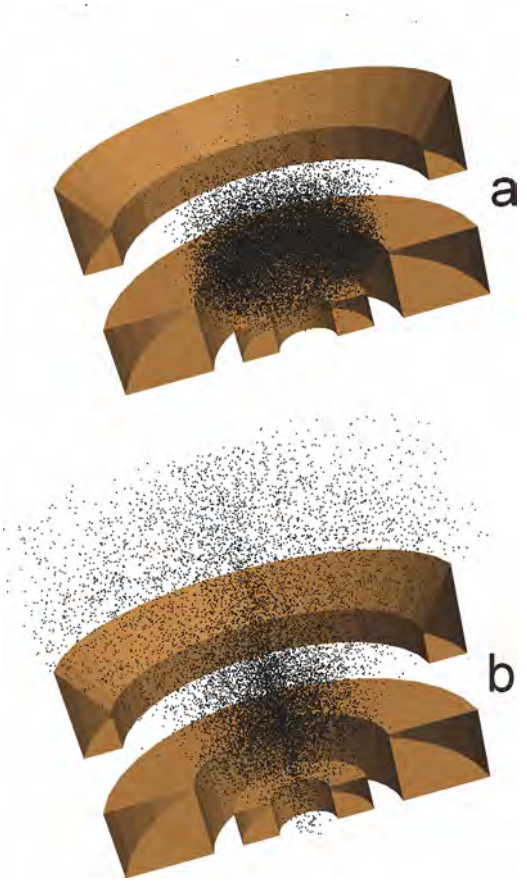

FIG. 6. Electron and ion phase space distributions (a – electron and b – ion).

variation with discharge voltage. They both exhibit a maximum value at about 900 V, indicating the maximum ionization efficiency at this voltage. The feature shown in Figs. 3 and 8 can be attributed to the cross section variation with electron energy (Fig. 5). The simulation shows that at 900 V, the maximum electron energy is 349.5 eV, the minimum electron energy is 0.006 eV, and the average energy for all electrons is 31.5 eV.

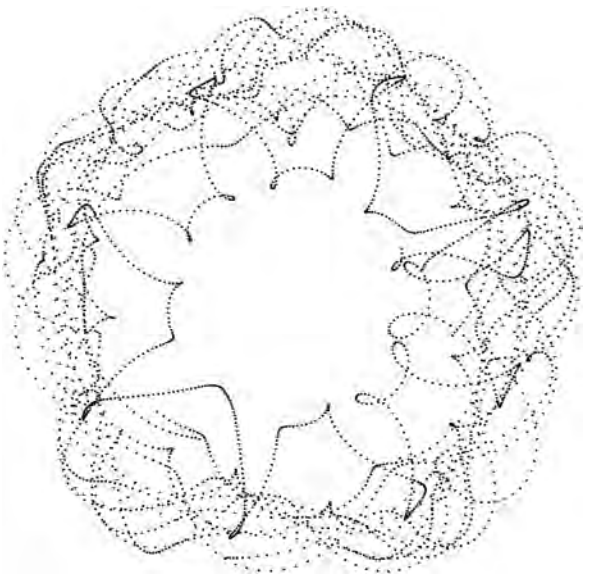

FIG. 7. Drift of electrons in the anode layer hall plasma accelerator.

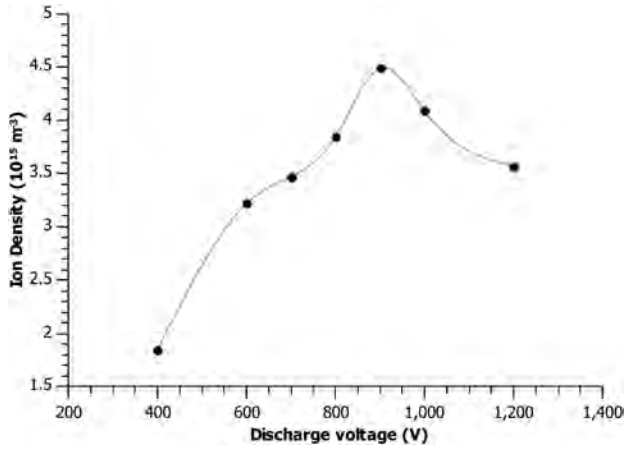

FIG. 8. Ion density versus discharge voltage in the simulation.

The motion of the electrons in a crossed-field has two components: gyration in a Lorentz transformed static magnetic field and uniform motion called hall drift.[26,27] By considering a new coordinate K' moving with a velocity $\vec{u}$ with respect to the original frame, we choose $\vec{u}$ as

$$\vec{u} = \frac{\vec{E} \times \vec{B}}{B^2}. \tag{1}$$

By making Lorentz transformation for electric field $\vec{E}$ and magnetic field $\vec{B}$, we get $\vec{E}'$ and $\vec{B}'$ in coordinate K' as[26,27]

$$\begin{aligned} \vec{E}' &= \gamma(\vec{E} + \vec{u} \times \vec{B}) = 0 \\ \vec{B}' &= \frac{1}{\gamma}\vec{B}. \end{aligned} \tag{2}$$

Here, γ is the Lorentz factor and after transformation, the magnetic field $\vec{B}'$ in frame K' is in the same direction as $\vec{B}$. The electric field $\vec{E}'$ is 0 and only the magnetic field $\vec{B}'$ is applied to the electrons. The motion of an electron is only by gyration in K' and the speed is $|\vec{u}|$ (for an original static electron). Combining the velocity $\vec{u}$, we can get the hall drift.

For an electron moving with a velocity $\vec{v}_1$ in K' and K' moving with a velocity $\vec{v}_2$ in K, the kinetic energy is

$$\varepsilon = \frac{1}{2}m(\vec{v}_1 + \vec{v}_2)^2 = \frac{1}{2}m|\vec{v}_1|^2 + \frac{1}{2}m|\vec{v}_2|^2 + m(\vec{v}_1 \cdot \vec{v}_2). \tag{3}$$

Here, we need the time average energy of an electron. In the present problem, the motion of an electron in K' is gyration, and so the time average of $m(\vec{v}_1 \cdot \vec{v}_2)$ is 0 and $|\vec{v}_1|$ is $|-\vec{u}|$. Consequently, $|\vec{v}_1|$ is equal to $|\vec{v}_2|$ and in short, the electron energy is governed by $\vec{u} = \frac{\vec{E}\times\vec{B}}{B^2} = \frac{E}{B}$. Furthermore, the ionization cross section and ionization efficiency are determined by the electromagnetic field. According to Fig. 5, the maximum ionization cross section appears when the electron energy is in the range of 45–110 eV. We can adjust the electromagnetic field to attain the maximum ionization cross section for maximum ionization efficiency.

Generally, the original energy of an electron is not 0, but it is still very small relative to the proper energy 45–110 eV. Thus, the non-zero energy of a newly ionized electron does not change the governance of E/B on the electron energy significantly. We know that the hall drift speed contributes to half of the time average energy of an electron based on formula (3). For an electron with energy 45–110 eV in the crossed field, the drift velocity is 2.81×10^6 m/s to 4.40×10^6 m/s, meaning that the appropriate E/B is in the range of 2.81×10^6 m/s to 4.40×10^6 m/s. In the plasma accelerator described in this paper, the magnetic field at the anode surface is 105 G and the electric field needed is 2.95×10^4 to 4.62×10^4 V/m. The electric field obtained from simulation is 3.75×10^4 V/m at 900 V. It is in the range of appropriate electric field. When the discharge voltage is increased, the electric field in the magnetized anode layer goes up and so does the ionization cross section. After the electric field reaches the proper E range, the area which has the proper electric field will increase as the voltage is increased. It increases the volume of the ionization layer. After the threshold voltage of 900 V, the opposite process is observed. The area which has the proper electric field diminishes and so does the ionization cross section due to the large E/B. Therefore, changing the electromagnetic field configuration will affect two factors: (a) E/B that can influence the ionization cross section and ionization efficiency and (b) the area which has the proper E/B in magnetized layer. Both of these factors can affect the discharge current.

We have only considered argon in this work. For other gases, the correlation between the electron energy and ionization cross section is the most important issue. All the others gases exhibit a similar behavior as that shown in Fig. 5 due to the basic physical process, that is, the interaction between the de Broglie wavelength of electrons and atoms. Different atoms have different dimensions and so the proper electron energy may be different.

V. CONCLUSION

In the anode layer hall plasma accelerator, a drop in the discharge current is observed with rising discharge voltage. This phenomenon is corroborated by 3D particle-in-cell simulation with respect to ion density. Simulation reveals a threshold discharge voltage of 900 V which is the same value determined experimentally. This is related to the correlation between the electron energy and ionization cross section. Lorentz transformation analysis discloses that the time average energy of an electron in the crossed-field discharge is governed by E/B and increasing the discharge voltage increases the ionization cross section. However, when the E/B exceeds the threshold value, the ionization cross section diminishes. For argon, the proper E/B is 2.81×10^6 m/s to 4.40×10^6 m/s. In a practical discharge, the voltage variation affects the discharge current by two factors, namely the ionization cross section and area which has proper E/B in the magnetized anode layer. The current drop observed experimentally is the macroscopic expression of the ionization cross section change with electron energy. For a different working gas, knowledge about the correlation between the electron energy and ionization cross section is necessary in order to determine the proper E/B.

ACKNOWLEDGMENTS

This work was supported by the National Natural Science Foundation of China under Grant No.10975050 and Hong Kong Research Grants Council (RGC) Special Equipment Grant (SEG) No. CityU SEG_CityU05.

[1]H. R. Kaufman, AIAA J. **23**, 78 (1985).
[2]V. V. Zhurin, H. R. Kaufmann, and R. S. Robinson, Plasma Sources Sci. Technol. **8**, R1 (1999).
[3]A. Smirnov, Y. Raitses, and N. J. Fisch, Phys. Plasmas **14**, 057106 (2007).
[4]A. Anders, Surf. Coat. Technol. **200**, 1893 (2005).
[5]H. R. Kaufman, R. S. Robinson, and R. I. Seddon, J.Vac. Sci. Technol. A **5**, 2081 (1987).
[6]V. Dudnikov and A. Westner, Rev. Sci. Instrum. **73**, 729 (2002).
[7]R. L. C. Wu, W. Lanter, J. Wrbanek, and C. Dejoseph, Surf. Coat. Technol. **140**, 35 (2001).
[8]D. A. Kotov, Rev. Sci. Instrum. **75**, 1934 (2004).
[9]G. T. West and P. J. Kelly, J. Vac. Sci. Technol. A **24**, 334 (2006).
[10]G. T. West and P. J. Kelly, Thin Solid Films **502**, 55 (2006).
[11]E. Y. Choueiri, Phys. Plasmas **8**, 5025 (2001).
[12]M. Keidar, I. D. Boyd, and I. I. Beilis, Phys. Plasmas **8**, 5315 (2001).
[13]L. Dorf, V. Semenov, and Y. Raitses, Appl. Phys. Lett. **83**, 2551 (2003).
[14]F. Taccogna, S. Longo, M. Capitelli, and R. Schneider, Contrib. Plasma Phys. **47**, 635 (2007).
[15]K. Komurasaki and Y. Arakawa, J. Propul. Power **11**, 1317 (1995).
[16]I. D. Boyd and J. T. Yim, J. Appl. Phys. **95**, 4575 (2004).
[17]E. Sommier, M. K. Scharfe, N. Gascon, M. A. Cappelli, and E. Fernandez, IEEE Trans. Plasma Sci. **35**, 1379 (2007).
[18]M. Keidar, I. D. Boyd, and I. I. Beilis, Phys. Plasmas **11**, 1715 (2004).
[19]A. Ducrocq, J. C. Adam, A. Héron, and G. Laval, Phys. Plasmas **13**, 102111 (2006).
[20]D. L. Tang, S. H. Pu, L. S. Wang, X. M. Qiu, and P. K. Chu, Rev. Sci. Instrum. **76**, 113502 (2005).
[21]D. L. Tang, L. S. Wang, S. H. Pu, C. M. Cheng, and P. K. Chu, Nucl. Instrum. Methods Phys. Res. B **257**, 796 (2007).
[22]D. L. Tang, J. Zhao, L. S. Wang, S. H. Pu, C. M. Cheng, and P. K. Chu, J. Appl. Phys. **102**, 123305 (2007).
[23]A. Kieckhafer and L. B. King, J. Propul. Power **23**, 21 (2007).
[24]R. C. Wetzel, F. A. Baiocchi, T. R. Hayes, and R. S. Feund, Phys. Rev. A **35**, 559 (1987).
[25]H. C. Straub, P. Renault, B. G. Lindsay, K. A. Smith, and R. F. Stebbings, Phys. Rev. A **52**, 1115 (1995).
[26]J. D. Jackson, *Classical Electrodynamics*, 3rd ed. (Wiley, New York, 1998), p. 586.
[27]R. Sugaya, Phys. Plasmas **10**, 3939 (2003).

Response to "Comment on 'Three-dimensional numerical investigation of electron transport with rotating spoke in a cylindrical anode layer Hall plasma accelerator'" [Phys. Plasmas 20, 014701 (2013)]

D. L. Tang,[1,a)] S. F. Geng,[1,2] X. M. Qiu,[1] and Paul K. Chu[2]
[1]*Southwestern Institute of Physics, Chengdu 610041, China*
[2]*Department of Physics and Materials Science, City University of Hong Kong, Tat Chee Avenue, Kowloon, Hong Kong*

(Received 5 November 2012; accepted 13 December 2012; published online 18 January 2013)

The numerical simulation described in our paper [D. L. Tang *et al.*, Phys. Plasmas **19**, 073519 (2012)] shows a rotating dense plasma structure, which is the critical characteristic of the rotating spoke. The simulated rotating spoke has a frequency of 12.5 MHz with a rotational speed of $\sim 1.0 \times 10^6$ m/s on the surface of the anode. Accompanied by the almost uniform azimuthal ion distribution, the non-axisymmetric electron distribution introduces two azimuthal electric fields with opposite directions. The azimuthal electric fields have the same rotational frequency and speed together with the rotating spoke. The azimuthal electric fields excite the axial electron drift upstream and downstream due to the additional E_θ *x* B field and then the axial shear flow is generated. The axial local charge separation induced by the axial shear electron flow may be compensated by the azimuthal electron transport, finally resulting in the azimuthal electric field rotation and electron transport with the rotating spoke. © *2013 American Institute of Physics*. [http://dx.doi.org/10.1063/1.4773896]

We appreciate the comments[1] by Ellison *et al.* on our paper[2] on some discussion about the numerical results of the rotating spoke phenomenon in a cylindrical anode layer plasma accelerator. They suggest that the oscillation behavior described in Ref. 2 is different from the typical rotating spoke phenomenon by experiments. The comments by Ellison *et al.* are based on two queries of the numerical study in Ref. 2. First, the rotation speed and frequency are too large and second, they think the simulated discharge in Ref. 2 is not self-sustained.

The numerical investigation in Ref. 2 shows a rotating, non-axisymmetric electron distribution in a cylindrical anode layer Hall plasma accelerator. This phenomenon has been observed from not only Hall plasma accelerator experiments[3–7] but also magnetron sputtering devices based on the discharge in the E *x* B field.[8,9] Accompanied by the almost uniform azimuthal ion distribution, the non-axisymmetric electron distribution introduces the local charge separation and two azimuthal electric fields with opposite directions in our simulation. The azimuthal electric fields excite the axial electron drift upstream and downstream due to the additional E_θ *x* B field and then the axial shear flow is generated. Anders *et al.*[10] have also reported an axial electron jet driven by E_θ *x* B in magnetron sputtering. The azimuthal electric fields have the same rotational frequency of 12.5 MHz with the rotating spoke since they are tied to the non-axisymmetric electron distribution. The frequency 12.5 MHz means different rotational speeds according to the radial distance from the position to the central axis due to the cylindrical structure. On the anode surface, which is almost the outer boundary of the rotating spoke, the rotational speed is $\sim 1.0 \times 10^6$ m/s. In this position, the axial electric field is ~470 V/cm and radial magnetic field is 175 G. They are consistent with the experimental measurement in Ref. 11 which reports an electric field of ~500 V/cm with magnetic field 200 G. The rotational speed of $\sim 1.0 \times 10^6$ m/s is ~37% of the drift speed determined by E/B on the anode surface. Meanwhile, the azimuthal electric filed E_θ also has the rotational speed of $\sim 1.0 \times 10^6$ m/s together with the rotating spoke. As described in Ref. 12, Lundin *et al.* performed a measurement of the azimuthal electric field in high power impulse magnetron sputtering. The result shows a rotating azimuthal electric field with a frequency of 2.35 MHz. By taking into account that the probe position is radially ~0.04 m away from the center of the target, the rotational speed is about 5.9×10^5 m/s which is also far more than the rotational speed $\sim 10^3$ m/s suggested by the previous rotating spoke experiments in Hall thrusters.[3–7]

Experimentally, small quantities of seed electrons appear accidentally, for example, due to cosmic rays. When a strong enough electric field is applied, electron avalanche begins followed by discharge.[13] In the cylindrical anode layer Hall plasma, the discharge is initiated by the seed electrons mentioned above. So it does not need an artificial electron source to start the discharge and the high ionization efficiency keeps the discharge self-sustained. Furthermore, in the simulation, the seed electrons are used to initiate the discharge. The ionization mechanism has been incorporated into the model, and new ions and electrons can be generated because of ionization. The simulated discharge in Ref. 2 is self-sustained even when there is no an external electron source.

In summary, we think the critical feature of the rotating spoke is the dense plasma structure. As shown in Ref. 2, the simulation results show the rotating, non-axisymmetric

a)Author to whom correspondence should be addressed. Electronic mail: tangdeli@263.net.

 © 2013 American Institute of Physics

electron distribution in a cylindrical anode layer Hall plasma accelerator. Accompanied by the almost uniform azimuthal ion distribution, the non-axisymmetric electron distribution introduces two azimuthal electric fields with opposite directions. The azimuthal electric fields excite the axial electron drift upstream and downstream due to the additional E_θ *x B* field and then the axial shear flow is generated. The axial local charge separation induced by the axial shear electron flow may be compensated by the azimuthal electron transport, finally resulting in the azimuthal electric field rotation and electron transport with the rotating spoke.

This work was supported by the National Natural Science Foundation of China under Grant No. 10975050 and Hong Kong Research Grants Council (RGC) Special Equipment Grant (SEG) No. CityU SEG_CityU05.

[1]C. L. Ellison, K. Matyash, J. Parker, Y. Raitses, and N. J. Fisch, Phys. Plasmas **20**, 014701 (2013).
[2]D. L. Tang, S. F. Geng, X. M. Qiu, and P. K. Chu, Phys. Plasmas **19**, 073519 (2012).
[3]G. S. Janes, Phys. Fluids **9**, 1115 (1966).
[4]P. J. Lomas and J. D. Kilkenny, Plasma Phys. **19**, 329 (1977).
[5]E. Chesta, C. M. Lam, N. B. Meezan, D. P. Schmidt, and M. A. Cappelli, IEEE Trans. Plasma Sci. **29**, 582 (2001).
[6]J. B. Parker, Y. Raitses, and N. J. Fisch, Appl. Phys. Lett. **97**, 091501 (2010).
[7]C. L. Ellison, Y. Raitses, and N. J. Fisch, Phys. Plasmas **19**, 013503 (2012).
[8]T. Ito and M. A. Cappelli, IEEE Trans. Plasma Sci. **36**, 1228 (2008).
[9]T. Ito and M. A. Cappelli, Appl. Phys. Lett. **94**, 211501 (2009).
[10]A. Anders, P. Ni, and A. Rauch, J. Appl. Phys. **111**, 053304 (2012).
[11]K. Komurasaki, S. Yokota, S. Yasui, and Y. Arakawa, in *40th AIAA/ASME/SAE/ASEE Joint Propulsion Conference and Exhibit, Fort Lauderdale, Florida, 11–14 July* (2004), Paper No. AIAA-2004-3954.
[12]D. Lundin, U. Helmersson, S. Kirkpatrick, S. Rohde, and N. Brenning, Plasma Sources Sci. Technol. **17**, 025007 (2008).
[13]Y. P. Raizer, *Gas Discharge Physics* (Springer-Verlag, Berlin, 1991), p. 128.